STATE OF THE CLIMATE IN 2010

J. Blunden, D. S. Arndt, and M. O. Baringer, Eds.

Associate Eds. H. J. Diamond, A. J. Dolman, R. L. Fogt, B. D. Hall, M. Jeffries, J. M. Levy, J. M. Renwick, J. Richter-Menge, P. W. Thorne, L. A. Vincent, and K. M. Willett

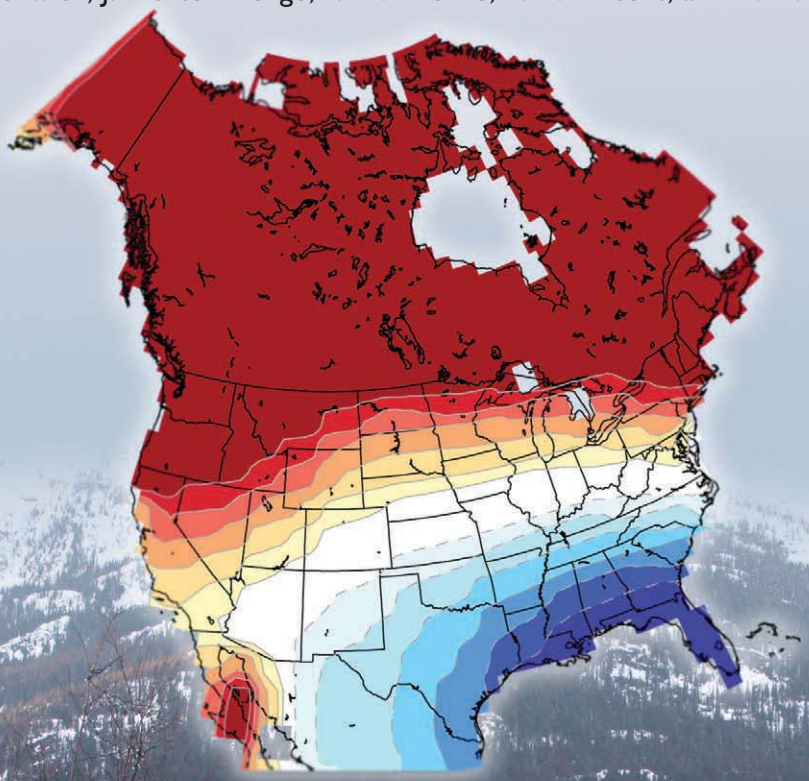

Special Supplement to the
Bulletin of the American Meteorological Society
Vol. 92, No. 6, June 2011

STATE OF THE CLIMATE IN 2010

roughly 20° and 25° in latitude are signatures of the predominance of evaporation over precipitation. Conversely, in most regions where climatological surface salinities are relatively fresh, such as the high latitudes and the Inter Tropical Convergence Zones (ITCZs), precipitation generally dominates over evaporation.

The 2010 SSS anomalies from WOA 2001 (Fig. 3.12a) reveal some large-scale patterns that also hold in 2004 through 2009. The regions around the subtropical salinity maxima are mostly salty with respect to WOA 2001. Most of the high-latitude climatologically fresh regions appear fresher than WOA 2001, including most of the Antarctic circumpolar current near 50°S and the subpolar gyre of the North Pacific. These patterns are consistent with an increase in the hydrological cycle (that is, more evaporation in drier locations and more precipitation in rainy areas), as seen in simulations of global warming. These simulations suggest this signal might be discernible over the last two decades of the 20th century (Held and Soden 2006), consistent with the multiyear nature of these anomalies. While anomalous ocean advection could influence the SSS pattern over decadal time scales, changes observed at the local extrema are presumably relatively insensitive to such effects. The analysis presented here for SSS anomalies is supported by others: difference of maps of 2003–07 Argo data and historical 1960–89 ocean data prepared in the same fashion show a similar pattern (Hosoda et al. 2009), as do estimates of linear trends from 1950 to 2008 (Durack and Wijffels 2010; see Sidebar 3.1 for further discussion, including interior ocean trends).

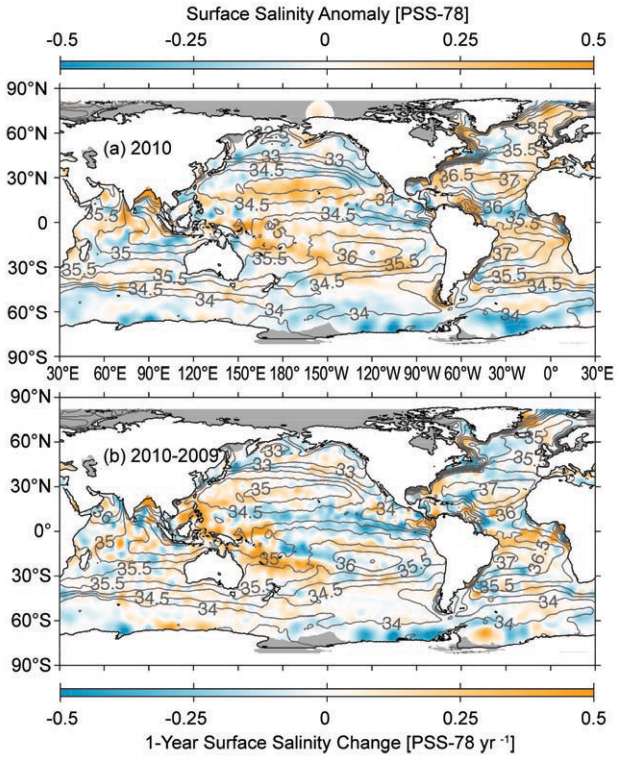

Fig. 3.12. (a) Map of the 2010 annual surface salinity anomaly estimated from Argo data [colors in 1978 Practical Salinity Scale (PSS-78)] with respect to a climatological salinity field from WOA 2001 (gray contours at 0.5 PSS-78 intervals). (b) The difference of 2010 and 2009 surface salinity maps estimated from Argo data [colors in PSS-78 yr^{-1} to allow direct comparison with (a)]. Gray areas are too data-poor to map. While salinity is often reported in practical salinity units (PSU), it is actually a dimensionless quantity reported on the PSS-78.

In contrast to the other high latitude areas, the subpolar North Atlantic and Nordic seas in 2010 are mostly anomalously salty (except east of Greenland) with respect to WOA 2001 (Fig. 3.12a), as they have been since at least 2004 (see previous *State of the Climate* reports). On the basin scale the North Atlantic loses some freshwater to the atmosphere whereas the North Pacific gains some (Schanze et al. 2010), thus the changes here may again be consistent with an increased hydrological cycle. In addition, the salty anomaly in this region is consistent with a stronger influence of subtropical gyre waters in the northeastern North Atlantic in recent years coupled with a reduced extent of the subpolar gyre (Häkkinen et al. 2011).

Sea surface salinity changes from 2009 to 2010 (Fig. 3.12b) strongly reflect 2010 anomalies in precipitation (Plate 2.1g), as well as year-to-year changes in evaporation, with the latter being closely related to latent plus sensible heat flux anomalies (Fig. 3.9b). Advection by anomalous ocean currents (Fig. 3.19) also plays a strong role in year-to-year variability of sea surface salinity. For instance, the western equatorial Pacific became considerably saltier from 2009 to 2010 while the central-eastern equatorial Pacific became fresher (Fig. 3.12b). This shift is likely partially owing to advection of salty water from the east by the anomalously westward surface currents on the Equator during that time, but an eastward shift in convection and precipitation in the equatorial Pacific during the strong El Niño in boreal winter 2009/10 also plays a large role. This pattern appears only partly compensated by the onset of La Niña later in 2010. The portion of the southwestern tropical region that became saltier in 2010 relative to 2009 may also have changed partly owing to anomalous westward surface currents. The eastern Pacific and Atlantic ITCZs also became fresher during this time period,

at least partly owing to anomalously strong precipitation in these regions during 2010. Anomalous vertical advection may also play a role in these changes, but is not analyzed here. There are strong correspondences between the surface salinity changes from 2009 to 2010 and subsurface changes over the same period (Figs. 3.14–3.16), with some of the surface changes apparently penetrating deep into the water column, suggesting influences of shifting ocean currents and fronts.

Trends from 2004 through 2010 are estimated by local linear fits to annual average SSS maps (Fig. 3.13a). The ratio of these trends to their 95% significance are also assessed (Fig. 3.13b). The starting year is 2004 because Argo coverage became near global then. The most striking trend patterns are in the Pacific. Saltier surface values in the western and central tropical Pacific extend into the eastern Pacific subtropics in both hemispheres. A strong freshening also occurs in the western subtropics of each hemisphere in the Pacific and the far western tropical Pacific, extending into the Indian Ocean northwest of Australia.

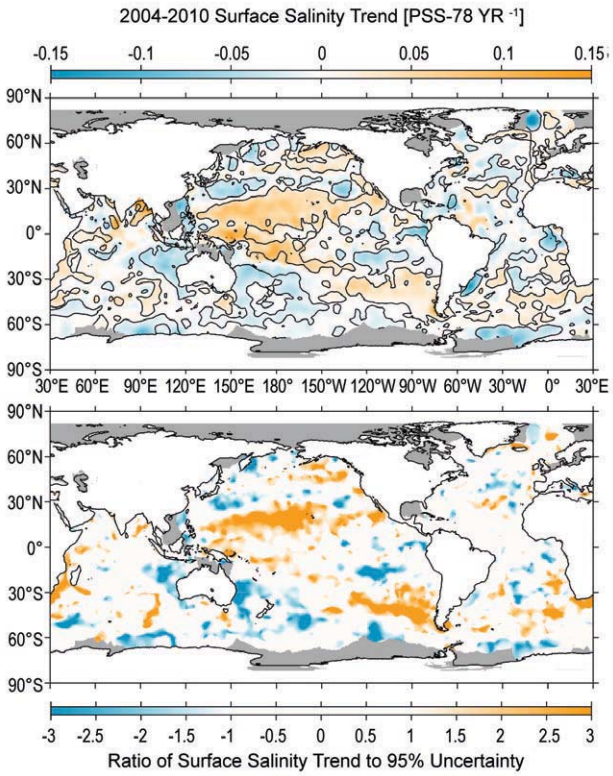

Fig. 3.13. (a) Map of local linear trends estimated from annual surface salinity anomalies for the years 2004 through 2010 estimated from Argo data (colors in PSS-78 yr^{-1}). (b) Signed ratio of the linear trend to its 95% uncertainty estimate, with increasing color intensity showing regions with increasingly statistically significant trends. Gray areas are too data-poor to map.

Large-scale freshening is also evident in the tropical Southeast Pacific. These recent trends differ from the 50-year trends discussed in the salinity sidebar of this chapter. These differences are not surprising given the very different time periods over which the trends are computed.

f. Subsurface salinity—S. Levitus, J. Antonov, T. Boyer, J. Reagan, and C. Schmid

Levitus (1989a, 1989b, 1989c), Antonov et al. (2002), Boyer et al. (2005), and Durack and Wijffels (2010) documented basin-scale changes of salinity for all or part of the world ocean on interpentadal or interdecadal time scales. Salinity changes reflect changes in the Earth's hydrological cycle and also contribute to change in sea level and ocean currents (Levitus 1990; Greatbatch et al. 1991; Sidebar 3.1).

The World Ocean Database 2009 (Boyer et al. 2009) updated through December 2010 has been used as the source of subsurface salinity data used in the analyses of 2009 and 2010 and climatological salinity conditions presented here. For 2009–10 it is primarily data from Argo profiling floats (approximately 109 000 profiles) that extend as deep as 2000 m and provide near-global coverage for the region within 60° of the Equator. Data from the TAO/TRITON, PIRATA, and RAMA arrays of tropical moored buoys provide important data in the upper 500 m of the water column. Approximately 13 000 ship-based conductivity/temperature/depth casts and 52 635 glider casts (these were highly localized in space) were also used. Final quality control has not been performed on some of the most recent observations used here, but it is not believed that additional quality control will substantially affect the results presented here. All data are available at http://www.nodc.noaa.gov.

The analysis procedure is as follows. First, monthly global analyses of salinity anomalies at standard depth levels from the sea surface to 2000 m depth are computed for years 2009 and 2010. For initial fields in the objective analyses the monthly salinity climatologies from the World Ocean Atlas 2009 (WOA09; Antonov et al. 2010) are used. Then observed data averaged on a 1° square grid at each standard depth are subtracted from the appropriate 1° climatological monthly mean. The next step is to objectively analyze (Antonov et al. 2010) these anomaly fields to generate a monthly anomaly field with an anomaly value defined at each grid point. The monthly anomaly fields are time averaged at each depth and gridpoint to define an annual mean anomaly field for each

standard depth level. This is done for 2009 and 2010.

Subsurface changes in salinity for the three major basins of the world ocean are documented in two ways. The first is to zonally average the WOA09 climatology and the 2010 annual mean field for each basin and plot these difference fields as a function of depth and latitude for the upper 1000 m of each basin as in Figs. 3.14a, 3.15a, and 3.16a. Examining these figures allows documentation of the difference in salinity conditions between 2010 and the "long-term" mean as best as can be determined with the historical data available used to construct WOA09. We only document variability in the upper 1000 m where signals are the largest and the figures can clearly document the changes that have occurred. This does not imply that changes deeper than 1000 m have not occurred, especially for the Atlantic. The second way is to document changes between these two years by zonally averaging the 2009 annual mean field by basins and plotting the 2010 minus the 2009 fields. It should be noted that it is only the advent of the Argo profiling float observing system that allows such a computation.

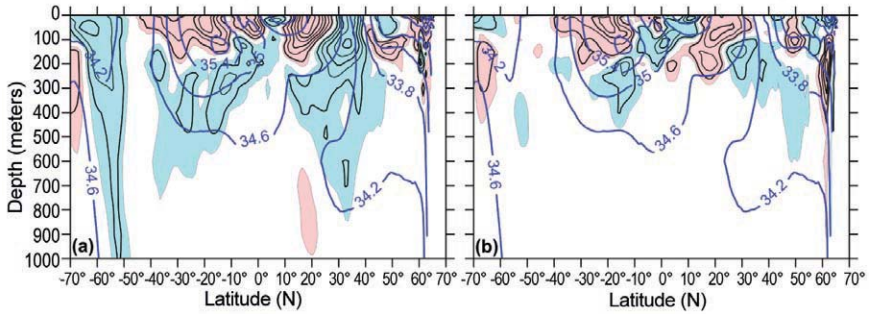

Fig 3.14. (a) Zonal mean 2010 salinity anomaly vs. latitude and depth for the Pacific Ocean. (b) Salinity anomaly 2010 minus 2009 vs. latitude and depth for the Pacific Ocean. For both plots blue shading is for areas of negative (fresh) anomaly < -0.01. Red shading is for areas of positive (salty) anomaly > 0.01. Contour interval shown for anomalies is 0.02. In the background (thick blue contours) is the zonally averaged climatological mean salinity. Contour intervals for the background are 0.4. All values are on the Practical Salinity Scale. WOA09 was used as the reference climatology for anomalies and for background means.

Figure 3.14a shows the 2010 minus climatology changes in salinity for the Pacific Ocean. There is a strong region of freshening (negative values) located in the 50°S–70°S region extending to 1000 m depth. In the 0°–45°S region there is a region of strong salinification (positive values) in the upper 200 m. This overlies a region of freshening that extends to about 700 m depth. In the 10°N–28°N region salinity has increased in the upper 125 m indicating an increase in the salinity of subtropical mode water (SMW; Yasuda and Hanawa 1997), an increase in the amount of SMW formed or both. In the 30°N–40°N region freshening occurred with the freshening extending as far south as 10°N at subsurface depths.

Figure 3.14b shows the 2010 minus 2009 changes in salinity for the Pacific Ocean. Most changes in subsurface salinity occur in the upper 400 m of this basin. At the sea surface, the 15°N–32°N region has become more saline with the positive anomaly extending south to about 10°N with increasing depth. This suggests changes in the properties of, or the amount of, SMW formed. A similar feature appears in the South Pacific centered around 20°S but with the more saline near-surface waters extending both further south and north. The subsurface high saline tongue extends northward to about 10°S. A surface freshening has occurred centered near 12°N that extends southward with increasing depth. This surface freshening may represent changes in rainfall in the Intertropical Convergence Zone (ITCZ). A relative maximum in freshening occurs centered at about 2°N at 125 m depth. This may not be directly related to changes in the ITCZ but could be linked to changes in upwelling or downwelling near the Equator which could be further linked to changes in the equatorial and tropical wind fields. Another region of subsurface freshening is centered near 12°S at 225 m depth. This might be related to changes in the tropical wind field.

Figure 3.15a shows the 2010 minus climatology changes in salinity for the Indian Ocean. Similar to the Pacific a region of freshening located in the 50°S–70°S region that extends to 1000 m depth. Immediately to the north of this feature a region (30°S–45°S) of salinification has occurred. Another region of salinification has occurred extending northward and downward from 30°S. Freshening has occurred in the 10°S–20°S region and salinification has occurred in the 10°S–12°N region.

Figure 3.15b shows the 2010 minus 2009 changes in salinity for the Indian Ocean. As in the Pacific, most changes in subsurface salinity occur in the upper 400 m of this basin. A notable exception occurs at 50°S. At 16°N and a depth of 50 m a relatively strong freshening occurred that extends to about 400 m depth. A possible explanation for this strong freshening at the

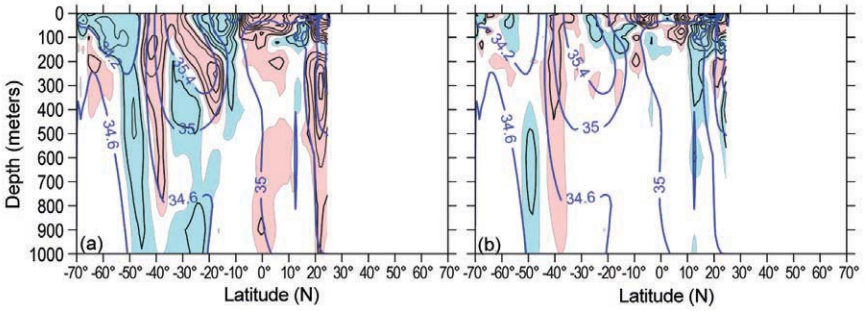

Fig 3.15. (a) Zonal mean 2010 salinity anomaly vs. latitude and depth for the Indian Ocean. (b) Salinity anomaly 2010 minus 2009 vs. latitude and depth for the Indian Ocean. For both plots blue shading is for areas of negative (fresh) anomaly < -0.01. Red shading is for areas of positive (salty) anomaly > 0.01. Contour interval shown for anomalies is 0.02. In the background (thick blue contours) is the zonally averaged climatological mean salinity. Contour intervals for the background are 0.4. All values are on the Practical Salinity Scale. WOA09 was used as the reference climatology for anomalies and for background means.

surface and deeper depths could be the ENSO impact on the Asian summer monsoon. In 2009 a strong El Niño occurred, whereas in 2010 conditions changed to a moderate-to-strong La Niña. It has been shown by Lim and Kim (2007) that during warm ENSO events (e.g., 2009), the Walker circulation in the tropical Pacific is displaced eastward resulting in higher sea level pressure in the western tropical Pacific and consequently results in subsidence over the western tropical Pacific and Indian Ocean. This pattern in turn, inhibits the ability for the monsoon to strengthen and thus less rainfall than normal falls (e.g., less freshening). Cold ENSO (e.g., 2010) events produce the reverse, with more lift in the Indian Ocean and western tropical Pacific resulting in stronger monsoons and more rainfall (e.g., more freshening). It should be noted that based on the work done by Kumar et al. (1999), this simple inverse relationship between ENSO and the Asian summer monsoon has weakened over the past two of decades. At 8°N a relatively strong increase in salinity has occurred extending to about 125 m with a similar increase in the 2°S–12°S region within the top 50 m of the water column. Another region of freshening is centered at 15°S and 100 m depth.

Figure 3.16a shows the 2010 minus climatology changes in salinity for the Atlantic Ocean. Similar to the Pacific and Indian oceans, a region of freshening occurs at high latitudes of the southern hemisphere extending to relatively deep depths (900 m). Immediately to the north is a region of salinification that is greater in magnitude than the corresponding region in the Indian Ocean. Unlike the North Pacific, the North Atlantic is characterized by an increase in salinity extending to several hundred meters depth. One exception is a very shallow region of freshening in the 0°–10°N region.

Figure 3.16b shows the 2010 minus 2009 changes in salinity for the Atlantic Ocean. Unlike the other two basins, changes in salinity have occurred to depths of 1000 m even on this one year time scale. This may be due in part to deep convection and the shifting position of large-scale fronts that have large vertical extension. Levitus (1989c) documented statistically significant large-scale changes at 1750 m depth for this basin on time scales of 20 years. Yashayaev and Loder (2009) discuss the variability of production of convectively formed Labrador Sea water. In the 60°N–70°N region, salinification has occurred that is strongest at the sea surface but extends vertically to 500 m depth. In the 50°N–60°N region,

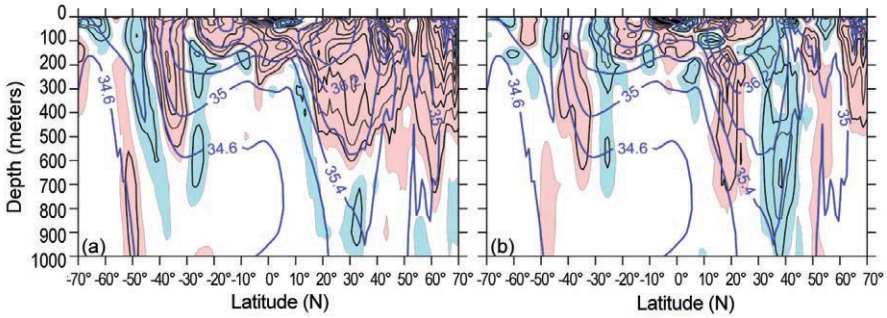

Fig 3.16. (a) Zonal mean 2010 salinity anomaly vs. latitude and depth for the Atlantic Ocean. (b) Salinity anomaly 2010 minus 2009 vs. latitude and depth for the Atlantic Ocean. For both plots blue shading is for areas of negative (fresh) anomaly < -0.01. Red shading is for areas of positive (salty) anomaly > 0.01. Contour interval shown for anomalies is 0.02. In the background (thick blue contours) is the zonally averaged climatological mean salinity. Contour intervals for the background are 0.4. All values are on the Practical Salinity Scale. WOA09 was used as the reference climatology for anomalies and for background means.

SIDEBAR 3.1: OCEAN SALINITY: A WATER CYCLE DIAGNOSTIC?—P. J. DURACK, S. E. WIJFFELS, AND N. L. BINDOFF

Present-day civilizations thrive in a wide range of temperatures at different latitudes across the Earth, but cannot cope without available freshwater. Changes to global water distribution are anticipated in the 21st century as anthropogenic climate change signatures become more apparent from natural variability of the climate system; future projections of surface moisture fluxes suggest that regions dominated by evaporation (over rainfall over the course of a year), will become drier, while regions dominated by rainfall (over evaporation) will become wetter (Allen and Ingram 2002; Held and Soden 2006; Meehl et al. 2007; Wentz et al. 2007; Seager et al. 2010). In water-stressed areas the human population and surrounding ecosystems are particularly vulnerable to decreasing or more variable rainfall due to climate change. Therefore, understanding probable future changes to the global water cycle are vital, as the projections of future climate show considerable changes to the water cycle are likely to significantly impact much of the world's population.

The global oceans cover 71% of the global surface, experience 75%–90% of global surface water fluxes, and contain 97% of the global freshwater volume (Schmitt 1995). As the ocean and land surface warms, so will the lower troposphere, and the amount of water vapor it can carry increases; this simple effect is anticipated to drive a stronger water cycle, with arid regions becoming drier and wet regions wetter (Held and Soden 2006). As the oceans are the engine room of the global water cycle, ocean salinity changes can be used to provide an estimate of broad-scale global water cycle changes and their regional patterns. Here, we review some of the major progress in understanding observed global water cycle changes in the ocean since the publication of the IPCC Fourth Assessment Report (AR4; Bindoff et al. 2007).

Global surface salinity is strongly correlated with the spatial patterns of E-P [evaporation (E) minus precipitation (P)] in the climatological mean. This relationship—where regions of low salinity correspond with regions of low (or negative) E-P and regions of high salinity with high E-P—provide some confidence in using salinity as a marker of global water cycle changes. Over long-timescales, the ocean integrates and smoothes high frequency and spatially patchy E-P fluxes at the ocean surface and provides a smoothed salinity anomaly field that facilitates detection of large-scale changes.

Patterns of long-term changes to surface salinity are now available, based on both trend fits directly to ocean data (e.g., Freeland et al. 1997; Curry et al. 2003; Boyer et al. 2005; Gordon and Giulivi 2008; Durack and Wijffels 2010) and comparisons of Argo era (2003–present) modern- to historical-ocean climatologies (e.g., Johnson and Lyman 2007; Hosoda et al. 2009; Roemmich and Gilson 2009; von Schuckmann et al. 2009; Helm et al. 2010). The patterns of multidecadal salinity change from these analyses show remarkable similarities between the mean E-P field and mean salinity field (Fig. 3.17). Rainfall-dominated regions such as the western Pacific warm pool, for example, have undergone a long-term freshening, and arid regions in the subtropical, evaporation-dominated 'desert latitudes' have generally increased in salinity (e.g., Fig. 3.17b).

Observed surface salinity changes suggest that changes in the global water cycle have occurred. The mean surface salinity climatology and the pattern of multidecadal (50-year) linear surface salinity changes (Durack and Wijffels 2010) have a spatial correlation of 0.7 (Fig. 3.18). Using this spatial relationship the amount of salinity pattern amplification can be obtained, with these data implying an amplification of the mean ocean surface salinity pattern of 8.0% has occurred between 1950 and 2000 (Fig. 3.18). In order to enhance the signal-to-noise for pattern

Continues on next page

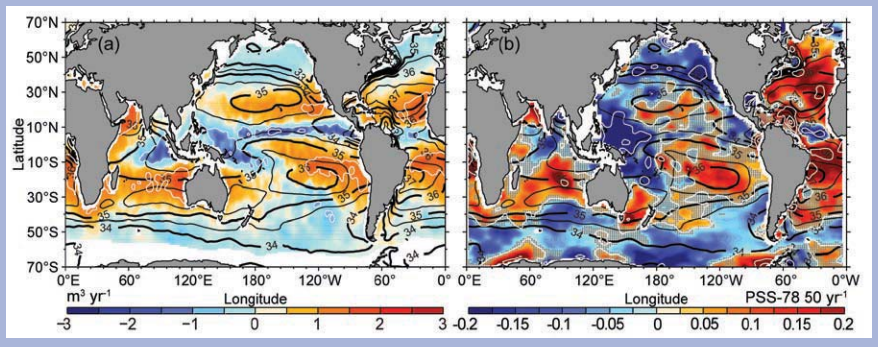

FIG. 3.17. (a) Ocean-atmosphere freshwater flux (E-P; $m^3\ yr^{-1}$) averaged over 1980–93 (Josey et al. 1998). Contours every 1 $m^3\ yr^{-1}$ in white. (b) The 50-year linear surface salinity trend (PSS-78 50 yr^{-1}). Contours every 0.25 (PSS-78) are plotted in white. On both panels, the 1975 surface mean salinity is contoured black [contour interval 0.5 (PSS-78) for thin lines, 1 for thick lines]. Due to limited observational E-P coverage a direct 1950–2000 climatology is not currently available, however the field produced by Josey et al. 1998 closely matches climatological means developed from many varied products over differing time periods (e.g. da Silva et al. 1994; Schanze et al. 2010) and provide a very similar spatial E-P pattern of correspondence with surface climatological mean salinity. Reproduced from Durack and Wijffels (2010).